ISSN: 2277-3754
ISO 9001:2008 Certified
International Journal of Engineering and Innovative Technology (IJEIT)
Volume 4, Issue 1, July 2014

Growth of Zinc Oxide Nano-Rod Thin Film for Hemoglobin Biosensor Applications Prepared Using Sol-Gel and Aqueous Chemical Growth

Hanan ABD El Zaher ABD EL Wahab[a], Omar Nur[b], Magnus Willander[b,] Aida ABD EL Karim Salama[c], ABD El Menem El Saeid[c] and I. K. Battisha[a,]
[a]National Research Center (NRC), Solid State Physics Department, Dokky, Giza, Egypt
[b]Department of Science and Technology, Campus Norrköping, Linköping University, SE-60174, Norrköping, Sweden.
[c]Al Azhar university, Physics Department, Cairo, Egypt

ABSTRACT-ZnO nano-rods (NRs) thin films of wurtzite hexagonal phase were grown on gold coated glass substrates with diameter equal 68 nm. It where prepared using both sol gel (SG) and aqueous chemical growth (ACG) methods by two steps of preparation seed layers and nano-rod growth. The effect of increasing the seed layer annealing temperature from 150 up to 300^{o}C on the structural and morphological properties is evaluated using X-ray diffraction (XRD), scanning electron microscope (SEM) and Atomic force microscope (AFM). The potentiometric response of the Fe^{3+} sensor with functionalized ZnO nanorods versus Ag/AgCl reference electrode was found to be linear over both logarithmic $FeCl_3$ concentration range from 10^{-5} M up to 10^{-2} M and Hemoglobin aqueous solution concentration ranging from 0.078 M/L to 0.26 M/L.

Keywords: **Nano structures, thin films, Sol-gel growth, X-ray diffraction, Crystal structure.**

I. INTRODUCTION

Semiconductor nano-materials have been the subject of considerable research due to their unique properties that can be applied at various functional nano-devices. Among them, zinc oxide (ZnO) nano-materials such as nano-wires, nano-tube and nano-rods (NRs) have been receiving particular attention, where it show many valuable properties and various shapes of ZnO nano-structures that can relatively easily be synthesized by diverse methods. It can be used for the detection of chemical and biological species. Chemical sensor is one of the important potential applications of ZnO (NRs), it is of great commercial interest in environmental and bio-industries. A relevant literature survey [1-6] reveals that ZnO (NRs) show n-type semiconducting property and that their electrical transport is highly dependent on the adsorption/desorption nature of chemical species. ZnO has generated keen interest in biosensors due to its enormous properties such as their small size, being bio-safe, possesses polar surface and many other properties that facilitate chemical sensing. Moreover, ZnO is non-toxicity, chemical stability, electrochemical activity, and has high electron communication features. These features make ZnO one of the most promising materials for chemical and biological applications [7]. In addition, the diameters of these ZnO nano-rods are comparable to the size of the biological and chemical species being sensed, which intuitively makes them represent excellent primary transducers for producing electrical signals [8-10]. All these facts open up for possible sensitive extracellular ion measurements. The detection of biological and chemical species is central to many areas of healthcare and life sciences [11]. Major importance for detection is the signal transduction associated with selective recognition of a biological or chemical species of interest, as was previously reported [12, 13] Iron is a vital element in the human body and is taking effective role in oxygen transport, storage and also in electron transport. The enzymes which are taking part in the synthesis of amino acids, hormones and neurotransmitters need Fe^{3+}. There is around 10-15 mg of iron to be exhibited in the food daily intake, and studies report that the normal subjects assimilate around 10% of the amount of iron from the food [14]. Due to the deficiency of iron, the amount of red blood cells in the body reduces and can become a cause of anemia. In addition, the surplus amount of iron is stored in the heart, liver and other organs [15, 16] and this extra iron cannot be spontaneously released from the body, but it is stored as mentioned above and can put other organs at risk of impairment [17]. Moreover, excess or less iron compounds in the human body are also cancer causing factors [18]. It is therefore very important for clinical, environmental and industrial purposes to efficiently detect Fe^{3+}. There are many methods for iron ions detection such as atomic absorption spectroscopy (AAS) [19], inductively coupled plasma (ICP) [20] etc... But these methods have many limitations such as high cost and instability if a large number of samples analysis is needed [19, 20]. Moreover, the potentiometric based sensing method is simple, inexpensive, rapid and more reliable for ions detection analyzing. The current study focus on the fabrication and demonstration of ZnO thin film (NRs) based sensor, suitable for extracellular selective iron ions detection in $FeCl_3$ and in aqueous solution of Hemoglobin. For this purpose ZnO nano-rods (NRs) thin film is grown on the surface of gold coated glass substrate to produce electrochemical nano-sensors.

ISSN: 2277-3754
ISO 9001:2008 Certified
International Journal of Engineering and Innovative Technology (IJEIT)
Volume 4, Issue 1, July 2014

The grown ZnO NRs thin films have been used to develop sensitive and selective iron ion (Fe^{3+}) potentiometric sensor in extra-cellular environments.

II. EXPERIMENTAL WORK

ZnO nano-rod thin films were prepared in two stages (seed solution deposition and nano-rod growth) using both sol-gel and aqueous chemical growth methods, respectively. Substrate was cleaning prior to synthesis the ZnO (NRs) is one of the most paramount to obtain the desired morphology and quality of the material. The substrates were immersed in ethanol then ultrasonically cleaned for 15 minutes and then dried with compressed nitrogen blow. This process helps to remove dust and unwanted chemicals from the surface of the substrate and provides a clean surface which can be used for further procedure. The seed solution is used for the surface modification of the substrate which, provides nucleation sights for the growth of nano-structures and helps to enhance the density as well as the homogeneity of particles. In addition the seed solution provides a good control on the alignment and density of the nucleation points that affect the diameter of the synthesized nano-structures. Different solvents and precursors were used for the preparation of seed solution. A coating seed solution was prepared by dissolving zinc acetate dehydrate (Zn $(CH3COO)_2 \cdot 2H_2O$) in mixed solution of monothanola mine (NH2CH2CH2OH) MEA and 2-methoxyethanol at room temperature, however the molar ratio of MEA to zinc acetate was 1:1. The seed solution was stirred at 50°C for 2 h until yielding a clear and homogeneous solution. The mixed solutions were aged at room temperature for another 24 h. Then the solution was coated on the glass and gold coated glass substrates by using spin coater method with a speed of 3000 rpm for 30 sec. The mentioned process was repeated several time and dried in open air at room temperature and finally placed in pre-heated laboratory oven at 250^{o}C for annealing in order to decompose the zinc acetate dehydrate into ZnO nano-particles. After uniformly coating the substrates with ZnO seed layers, ZnO (NRs) were grown on it using aqueous chemical growth (ACG) method at low temperature 90 – 95^{o}C. ZnO nano-rods growth was achieved by immersing ZnO seed-layer in 150 mL of aqueous solution composed of 0.025 M zinc nitrate (Zn (NO3)2) and 0.025 M hexamethylenetetramine (HMT, C6H12N4) in a conventional flask. The reaction temperature was kept at 90 - 95^{0}C for 6 h. The position of the substrate inside the solution does affect much on the growth process however; the substrate is being placed in the solution with face toward the bottom of the beaker. Finally, the substrate were removed from the solution, then immediately rinsed in de-ionized water to remove any residual salt from the surface, and dried in air at room temperature. The resulting ZnO (NRs) structure was characterized by X-ray diffraction (XRD), scanning electron microscope (SEM) and atomic force microscope (AFM) for crystallinity and surface morphology, respectively. For extracellular iron ions measurements, the ZnO (NRs) is deposited on gold coated glass substrate with ionophore membrane thin layer by manual procedure. The ionophore membrane was prepared with the following composition, 18- crown- 6(18CE6) [Fluka], it was used for iron ion selectivity; While Dioctyl phenylphosphonate (DOPP) [Aldrich] was used as plasticizer. Polyvinylchloride (PVC) [Fluka] was used as the membrane matrix and tetrahydrofuran (THF) [Flika] was used as solvent. After preparing the ionophore solution, the ZnO gold coated glass substrate was dipped twice in it for 5 minutes until the membrane thin film is attached to the surface of the substrate and then dried it for 1-2 hours at room temperature. Generally all the sensors were kept at 4^{o}C when not in use. The proposed Fe^{3+} sensors were used as working electrode for the potentiometric measurements in both an electrolytic solution of ferric chloride ($FeCl_3$) with concentrations ranging from 10^{-6} M up to 10^{-2} M and in aqueous solutions of Hemoglobin with a concentration ranging from 0.078 M to 0.026 M, while, Ag/AgCl was acting as a reference electrode. The output voltage of this experiment for each concentration of the two mentioned solutions was recorded by using pH meter (model 3510Metrohm). X-ray diffraction (XRD) patterns were recorded by using a Philips X-ray diffractometer using monochromatic CuK□ 1 radiation of wavelength □ □ = 1.5418 Å from a fixed source operated at 40 kV and 30 mA. The crystallite size (G) is determined from the Scherrer' s equation G = K□ □ / D cos(□), where K is the Scherer constant, (0.9), □ □ is the wavelength and D is the peak full width (in radians) at half maximum (FWHM) intensity. The coarse and fine microstructures and the morphology of all the ZnO NRs thin films were depicted by using Field Emission Scanning electron microscope (FESEM) JEOL JSM-63o1F (SEM) and AFM. The SEM gives information on the surface morphology of the sample, which can help us to check whether the growth has taken place or not. The SEM produced 2 D image and reveals topographic filature of the sample, which allow us to examine the diameter, length, shape and density of the ZnO NRs. The AFM was used due to its several advantages over the SEM, while the AFM provides a three- dimensional profile. The sample viewed by SEM usually required meal/carbon coating to improve the conductivity of the surfaces in order to enhance the resolution, which would irreversibly change or damage the sample, while the samples can be directly measured by AFM without any preparation or pre-treatment. An expensive vacuum environment is always needed for proper operation in SEM. While, most AFM modes can work perfectly well in ambient air or even a liquid environment, which make it possible to study biological macromolecules and even living organisms. Nearly normal transmittance and reflectance spectra were done

ISSN: 2277-3754
ISO 9001:2008 Certified
International Journal of Engineering and Innovative Technology (IJEIT)
Volume 4, Issue 1, July 2014

by Jasco V-570 spectrophotometer, in wavelength range (0.2 -2.5 μm). The absorption coefficient (α) for all investigated samples is calculated. The film thickness is measured by using the tally-step instrument with an experimental error ± 3.5%. The recorded charts for transmittance measurements were at normal incidence, while reflectance measurements were performed at incident angle of 8°.

III. RESUTS AND DISCUSSION

The X- ray diffraction (XRD) analysis was performed on ZnO thin films both before and after the formation of nano-rods. Figure 1 (a, b & c) shows the X-ray diffraction patterns of ZnO nano-particle thin films as a (seed layer) prior to the nano-rods growth at different annealing temperature 100, 150 and 250^{o}C, respectively. ZnO amorphous phase appeared at lower temperature 100^{o}C, as shown in Figure 1 (a). Figure 1 (b and c) further indicated the growth orientations and crystal structure of ZnO (NRs) thin films by revealing emission peaks at 2Θ^{o} equal to 31.7, 34.45, 36.29, 47.39, 56.5, 62.59 and 68.2°, corresponding to (100), (002), (101), (102), (110), (103) and (112) preferred orientations, respectively. No other diffraction peaks impurities were detected, which testify that the substance deposited on the substrate only belongs to ZnO. All diffraction peaks can be indexed to ZnO with the hexagonal wurtizite structure, in comparison with the standard card of bulk ZnO with hexagonal structure, which corresponds to Card number [01-089-1397] [21]. Figure 1 (d) shows the XRD pattern of the ZnO (NRs) after growth on seed layer sintered at 250^{o}C for comparison between the nano-particle and (NRs) growth. Stronger and sharper diffraction peaks corresponding to ZnO hexagonal wurtizite structure were appeared. The sharper diffraction peak at 2 Θ^{o} equal to 34.45 corresponding to the (002) crystal plan indicated that the orientation growth of (NRs) along the C-axis direction is of ZnO wurtzite crystal, which is perpendicular to the substrate. Figure 2 shows the XRD patterns of the ZnO NRs thin films obtained at different annealing temperature of seed layer for 1 h. The principle peak at (002) can be observed and its relative intensity is increased obviously with an increase of temperature from 150 up to 250^{o}C, and reaches its highest point when the annealing temperature is at 250^{o}C. However with further annealing temperature increase up to 300^{o}C or above, besides the diffraction peak at (002), some other peaks at (100) and (101) can be also clearly observed and the relative intensity of the peak at (002) starts to decrease. The obtained XRD results indicate that the optimum annealing temperature needed to obtain highly preferred orientation ZnO thin films along (002) plane is at 250^{o}C and the ZnO thin film obtained at present conditions shows a wurtzite crystal structure. A possible explanation is as follows: The crystallization process can be considered as an equilibrium process of the atoms disordered thermal motion and ordered crystallization. Although the crystallization of the thin film has a trend of along (002) plane, the crystallization process at the beginning of the annealing temperature is random. With the annealing temperature increase, atoms with enough energy can get across the crystal boundary and the random crystallization becomes preferred orientation, provided that the annealing temperature is at a proper value, until arrive at a balance process where all the crystal grains grow along C axis. However, this balance cannot be arrived if either the annealing temperature is below or above the certain proper value, since the atoms' thermal motion energy is either too low to get across the crystal boundary or too high to maintain the balance. So there is an optimum temperature to maintain this balance and obtain the highly preferred orientation thin film and it is in our case at 250^{o}C.

Scanning electron microscope (SEM)

The seed layers surface morphology of high density ZnO (NRs) thin films grown on glass substrates with different annealing temperature were found to be vertically aligned and distributed uniformly with an average diameter of (60-95 nm), as shown in Figures (3-5) of SEM. The obtained SEM image in Fig.3 shows the seed layers ZnO (NRs) grown on glass substrate, at annealing temperature 150^{o}C. A rod-like shape with hexagonal cross section is obtained and primarily aligned along the c-axis (perpendicular to the substrate), which corresponds well with the result of XRD. Figure 4 shows the ZnO (NRs) grown on glass substrate, with seed layers at annealing temperature 250^{o}C, 3 layers (a), 6 layers (b) and 6 layers focusing view on the hexagonal structure (c). The obtained result indicated that the 6 layers sample is dens and highly oriented more than the 3 layers sample. A well hexagonal shape is observed as shown in Figure 4 (c). Figure 5 shows typical scanning electron microscopy (SEM) images of ZnO (NRs) grown on glass substrate, with seed layers at annealing temperature 300^{o}C with 3 layers (a) and 6 layers (b). The result indicated that the image in Figure 5 (b) is denser and highly oriented more than the image in Figure 5 (a), both figures gave the same rod shape appeared in Figure 3. The obtained results from Figs 4 and 5 indicated that the number of ZnO nano-particles seed layers deposited on the substrate will directly influence the formation of ZnO (NRs). The seed solution is used for the surface modification of substrate, which provides nucleation sights for the growth of nano-structures and helps to enhance the density as well as homogeneity of particles. The density of ZnO nano-particles on the substrate can be controlled by the number of spin coating layers. Therefore, adjusting the density of ZnO nano-particles on the substrate should be an effective way to control the diameter of the NRs. The SEM images in Figures 4 and 5, indicated that the diameter of ZnO (NRs) decreased by increasing ZnO nano-particles density [22]. On the other hand the orientation of ZnO (NRs) becomes better by increasing ZnO nano-particles density [23]. This result indicated that

ISSN: 2277-3754
ISO 9001:2008 Certified
International Journal of Engineering and Innovative Technology (IJEIT)
Volume 4, Issue 1, July 2014

the diameter of ZnO (NRs) mainly depends on the density of ZnO nano-particles [24]. The panoramic SEM images of ZnO (NRs) deposited on gold coated glass substrates both before and after coating with iron membrane was depicted in Fig.6 (a& b). The ZnO (NRs) AFM images prepared by low temperature (ACG) method are represented in Fig. (7). From the AFM images we observed that the surface morphologies proved the densification of the film and the grains are formed as nano-grains structures. The existence of this nano-grain structure is very important as the transport properties of these films are usually limited by recombination of the minority carriers at grain boundaries. The ZnO (NRs) three-dimensional surface morphology is represented in Fig 7 (b), it shows plicate structure that causes to unflatness of surface to appear**,** however porous aspect can be remarked. Figure 8 shows the absorbance spectra as a function of wavelength for the aligned ZnO (NRs) thin film, prepared at different temperature 150, 250 and 300^{o}C prepared by (ACG), at visible wavelengths (300-800 nm). The spectra indicated that it has high UV absorbance properties at wavelength below 400 nm. The sharp absorption edge observed around 380 nm for the film annealed at 150^{o}C was decreased by increasing the temperature up to 250 and then 300^{o}C. It is corresponded to the direct transition of electrons between the edges of the valance band and the conduction band. The normal reflectance and transmission measurements were given for the prepared ZnO NRs thin films. The absorption coefficient (α) and the band gap (Eg) for ZnO NRs thin films were determined by calculating (α) by a simple method from transmittance spectra using the following relation; T = exp [-α(λ)d], where T is the optical transmittance and d is the thickness of ZnO film. It is clear from Fig. 9. that at short wavelengths, a steep decrease was occurred in the absorption coefficient (α) around the absorption edge (at *Eg*) and that (α) is decreased by increasing the annealing temperature. This decrease might be due to the increase of the surface roughness caused by higher temperature. The optical energy band gap Eg was related to the absorption coefficient in accordance with the equation $(\alpha h\nu) = A(h\nu-Eg)^{p}$ as shown in Figure 10, where A is a constant, h is the Plank's constant and P is a constant that depends on the type of the electronic transitions. For allowed direct transition P is equal to 1/2. However P may also be equal to 3/2 for forbidden direct transition, 2 for indirect allowed transition and 3 for indirect forbidden transitions. It is well known that ZnO is a direct band gap semiconductor with hexagonal wurzite crystal structure, and has a wide band gap of 3.37 eV and large exciton binding energy of 60 meV [25-30]. We assume that the absorption coefficient $\alpha = (1/d)\ln(1/T)$, where T is the transmittance and d is the film thickness. Therefore the optical band gap was obtained by plotting $(\alpha h\nu)^2$ as a function of a photon energy (hν). Typical plots of $(\alpha h\nu)^2$ as a function of (hν) for ZnO NRs thin films fabricated by both sol-gel and ACG methods and annealed at different temperature at 150, 250 and 300^{o}C, respectively were shown in Figure 10. The intercept of the extrapolation to zero absorption with photon energy axis gave the values of the direct energy gap Eg. It is clear from these intercepts that the direct energy gap increases by increasing the annealing temperature of seed layer. It can be seen that the optical band gap exhibits a slight blue shift by increasing the temperature. This shift may be attributed to the changes of the quality of the films by increasing the annealing temperature. While by increasing annealing temperature, the stoichiometry of the ZnO NRs thin films is improved. i.e. the defect number decreases. The obtained results indicated that the energy band gab of ZnO NRs thin film, prepared by sol-gel technique and ACG is~ 3.625, 3.666 and 3.708 eV for thin film heated at 150, 250 and 300^{o}C, respectively. The obtained results indicated that the energy band gab was shifted upward in energy from 3.625 to 3.666 and then 3.708 eV by decreasing the diameter of nano-rods from the 95 up to 68 nm as a result of increasing the annealing temperature of seed layers as obtained from SEM. It is known that the energy band gap of the ZnO thin film could be affected by the residual strain defects and grain size confinement.

Response Time of the Functionalized ZnO Nanorods Iron Selective Electrode

Electrochemical measurements were carried out using two-electrodes configuration consisting of ZnO (NRs) as the working electrode and an Ag/AgCl as a reference electrode. The electrochemical response was observed until the equilibrium potential has reached and stabilized.

(a) Measuring of potential difference in $FeCl_3$ electrolytic solution.

We used our sample to study iron ion selectivity of ZnO (NRs) sensors using ionophore membrane coatings. The potentiometric response of the Fe^{3+} ions was studied in aqueous solutions of $FeCl_3$ with concentration ranging from 10^{-6} M to 10^{-2} M. The electrochemical cell voltage (electromotive force) changes when the composition of the test electrolyte solution was changed. These changes can be related to the concentration of iron ions in the test solution via a calibration procedure.

The construction of the cell potential of the developed Fe^{3+} sensor presented here can be shown by the diagram bellow:

Au |ZnO | membrane **|** $FeCl_3$ electrolytic solution || Cl-|AgCl | Ag

The cell voltage is a function of the concentration of the testing electrolyte solution. This means that the voltage changes due to the change in concentration of iron ion in the testing solution. We added 2 ml of 10^{-1} M of KNO_3 solution in each testing ferric chloride solution in order to adjust the ionic concentration inside the solution. We tested the selective Fe^{3+} sensor into 10^{-6} M iron electrolytic solution and we observed that the output response of the Fe^{3+} sensor was not stable. Then this Fe^{3+}

ISSN: 2277-3754
ISO 9001:2008 Certified
International Journal of Engineering and Innovative Technology (IJEIT)
Volume 4, Issue 1, July 2014

sensor was tested in 5×10^{-6} M and the proposed Fe^{3+} sensor responded with stable output response. Further we checked the response of the functionalized ZnO Fe^{3+} electrode into 10^{-5} M to 10^{-2} M, and observed that the Fe^{3+} sensor showed very stable output voltage for this concentration range. Fig.11. Shows the calibration curve of the logarithm concentration of Fe^{3+} in $FeCl_3$ solution versus the output voltage response by using gold coated glass substrate as a sensor. The proposed iron ion sensor has shown good linearity for a wide concentration range from 10^{-5}M to 10^{-2}M of iron ions. The results show that the electrode is highly sensitive to iron ions with a slope around 43.2mV/decade with a regression coefficient R^2 = 0.95.

(b) Measuring of potential difference in Hemoglobin aqueous solution.

We used our sample to study iron ion selectivity of ZnO (NRs) sensors using ionophore membrane coatings. The potentiometric response of the Fe^{3+} ions was studied in aqueous solutions of Hemoglobin with concentration ranging from 0.078 M to 0.026 M. The electrochemical cell voltage (electromotive force) changes when the composition of the test hemoglobin aqueous solution was changed. These changes can be related to the concentration of iron ions in the test solution via a calibration procedure. The construction of the cell potential of the developed Fe^{3+} sensor presented here can be shown by the diagram bellow:

Au |ZnO | membrane | Hemoglobin aqueous solution || Cl- |AgCl | Ag

The cell voltage is a function of the concentration of the testing Hemoglobin solution. This means that the voltage changes due to the change in concentration of iron ions in the testing solution. We checked the response of the functionalized ZnO Fe^{3+} electrode into 0.078 M/L to 0.26 M/L, and observed that the Fe^{3+} sensor showed very stable output voltage for this concentration range. Figure 12. Shows the calibration curve of the logarithm concentration of Fe^{3+} in Hemoglobin aqueous solution versus the output voltage response by using gold coated glass substrate as a sensor. The proposed iron ion sensor has shown good linearity for a wide concentration range from 0.078M/L to 0.26M/L of iron ion in the Hemoglobin aqueous solutions. The results show that the electrode is highly sensitive to iron ions with a slope around 42.3 mV/decade with a regression coefficient R^2 = 0.97.

IV. CONCLUSION

The sol gel and aqueous chemical growth methods were successfully used in preparing the two steps of the ZnO (NRs) thin films with Wurtzite hexagonal structure as revealed from XRD analysis. The ZnO (NRs) grown on glass substrate and silver wire were found to be vertically aligned and distributed uniformly with an average diameter of (60-95 nm). The AFM study depicted a plicate structure that causes to unflatness of surface to appear. The potentiometric response of the Fe^{3+} ions was studied in FeCl3 aqueous solutions with concentration ranging from 10^{-6} M. to 10^{-2} M. The presented iron biosensor based on ZnO (NRs) on Ag wire provides substantial advantage due its smaller size, cost efficiency and ease of fabrication. We used our sample to study iron ion selectivity of ZnO (NRs) sensors using ionophore membrane coatings. The proposed iron ion sensor has shown good linearity for a wide concentration range from 10^{-6} M to 10^{-2} M of iron ions. The results show that the electrode is highly sensitive to iron ions with a slope around 43.2±2.81 mV/decade with a regression coefficient R2 =0.95. While the calibration curve of the logarithm concentration of Fe^{3+} in Hemoglobin aqueous solution versus the output voltage response by using gold coated glass substrate as a sensor, is shown good linearity for a wide concentration range from 0.078M/L to 0.26M/L of iron ion in the Hemoglobin aqueous solutions. The results show that the electrode is highly sensitive to iron ions with a slope around 42.3 mV/decade with a regression coefficient R^2 = 0.97.

REFERENCES

[1] S. Wei, S. Wang, Y. Zhang, M. Zhou , j of Sensors and Actuators B., 192, 480– 487, (2014).

[2] G. H. Lee, j of Applied Surface Science. 259, 562– 565, (2012).

[3] M.Y. Soomro, I Hussain, N. Bano, S. Hussain, O. Nur and M. Willander, Applied Physics A. 106(1), 151-156, (2012).

[4] P. Li, H. Liu, F.X. Xu, Y. Wei, Mater. Chem. Phys., 112, 393–397, (2008).

[5] Y.F. Hsu, E.S.P. Leong, W.M. Kwok, Aleksandra B. Djurišić, S.F. Yu, D.L. Phillips, W.K. Chan, Opt. Mater., 31, 35–38, (2008).

[6] S.C. Lyu, Y. Zhang, H. Ruh, H.-J. Lee, H.-W. Shim, E.-K. Suh, C.J. Lee, Chem. Phys. Lett., 363, 134–138, (2002).

[7] M. H. Huang, S. Mao, H. Feick, H. Yan, Y. Wu, H. Kind, E. Weber, R. Russo, P. Yang, Science., 292, 1897-1899, (2001).

[8] J. C. Johnson, H.J. Choi, K. P. Knutsen, R. D. Schaller, P. Yang, R. J. Saykally, Nat. Mater., 1, 106-110, (2002).

[9] X. Duan, Y. Huang, R. Agarwal, C. M. Lieber, Nature (London)., 421, 241-245, (2003).

[10] P. Yang, H. Yan, S. Mao, R. Russo, J. Johnson, R. Saykally, N. Morris, J. Pham, R. He, H.J. Choi, Adv. Funct. Mater., 12, 323–331, (2002).

[11] C. J. Barrelet, A. B. Greytak, C. M. Lieber, Nano Lett., 4, 1981-1985, (2004).

[12] B. Shouli, C. Liangyuan, L. Dianqing, Y. Wensheng, Y. Pengcheng, L. Zhiyong, C.Aifan, C. C. Liu, Sensors and Actuators B.,146, 129–137, (2010).

[13] M. Willander, L. L. Yang, A. Wadeasa, S. U. Ali, M. H. Asif, Q. X. Zhao, O. Nur, J. Mater.Chem., 19, 1006-1018, (2009).

ISSN: 2277-3754
ISO 9001:2008 Certified
International Journal of Engineering and Innovative Technology (IJEIT)
Volume 4, Issue 1, July 2014

[14] N. ul H. Alvi, K. ul Hasan, M. Willander and O. Nour, Lighting Research and Technology, 43(3), 331-336, (2011).

[15] M.H. Huang, Y.Y. Wu, H. Feick, N. Tran, E. Weber, P.D. Yang, Adv. Mater.,13, 113–116, (2001).

[16] X.M. Sun, X. Chen, Z.X. Deng, Y.D. Li, Mater. Chem. Phys. 78 (2002) 99–104.

[17] Y.Ding, Z.L.Wang, Micron 40, 335–342, (2009).

[18] K.Khun, Z. H. Ibupoto, S. U. Ali, C. O. Chey, O. Nur and M. Willander. 24(3), 521-528, (2012).

[19] Y.L. Cao, W.Y. Pan, Z. Ying, D.Z. Jia, Actuator B 3 (2009) 23–28.

[20] M. M. Zareh, I. F. A. Ismail, M. H. A. El-Aziz, Electroanalysis., 22 (1), 1369-1375, (2010).

[21] H. A. Wahab, A. A. Salama, A. A. El-Saeid, O. Nur, M. Willander and I. K. Battisha,, J. of Results in Physics., 3, 46 – 51, (2013).

[22] Z. Liu, J. Ya and L.E, J. Solid state Electrochem., 14, 957-963, (2010).

[23] Wang, T. Y. Tseng, Y. R. Wang, C. Y. Wang and H.C. Lu, J. Ceramic. International. 35, 1255-1260, (2009).

[24] L. Yang, Q. Zhao, M. Willander and J. Yang, J. Crystal Growth., 311, 1046-1050, (2009).

[25] S. Wei, S. Wang, Y. Zhang, M. Zhou , j of Sensors and Actuators B., 192, 480– 487, (2014).

[26] G. H. Lee, j of Applied Surface Science., 259, 562– 565, (2012).

[27] P. Li, H. Liu, F.X. Xu, Y. Wei, Mater. Chem. Phys., 112, 393–397, (2008).

[28] Y.F. Hsu, E.S.P. Leong, W.M. Kwok, Aleksandra B. Djurišić, S.F. Yu, D.L. Phillips, W.K. Chan, Opt. Mater., 31, 35–38, (2008).

[29] S.C. Lyu, Y. Zhang, H. Ruh, H.-J. Lee, H.-W. Shim, E.-K. Suh, C.J. Lee, Chem. Phys. Lett., 363, 134–138, (2002).

[30] S. W. Xue, X. T. Zu, W. L. Zhou, H. X. Deng, X. X.iang, L. Zhang and H. Dang, J. of Alloys and compounds. 448, 21-26, (2008).

Figure captions:-

Fig. 1. (a, b,c & d) XRD of ZnO nano-particles (seed layer) before the growth of (NRs) prepared by spin coating sol gel method, heated at different temperature 100 (a), 150 (b), 250^{o}C (c), respectively. typical XRD of ZnO (NRs) prepared by aqueous chemical growth at 90^{o}C (d).

Fig. 2. XRD patterns of the ZnO NRs thin films prepared on seed layers under different annealing temperatures.

Fig. 3. Typical scanning electron microscopy (SEM) images of ZnO nano-rods grown on glass substrate, with seed layers at annealing temperature 150^{o} C.

Fig.4. Typical scanning electron microscopy (SEM) images of ZnO nano-rods grown on glass substrate, with seed layers at annealing temperature 250^{o} C (a) 3 layers (b) 6 layers and (c) 6 layers to focus on the hexagonal structure.

Fig.5. Typical scanning electron microscopy (SEM) images of ZnO nano-rods grown on glass substrate, with seed layers at annealing temperature 300^{o} C (a) 3 layers (b) 6 layers.

Fig. 6. Typical scanning electron microscopy (SEM) images of ZnO nano-rods grown on gold coated glass substrate (a) before coating with iron membrane, (b) after coating with iron membrane.

Fig.7. AFM images of ZnO (NRs) prepared by low temperature (ACG) method.

Fig.8. The absorbance of the ZnO (NRs) prepared at different temperature 150 ,250 and 300^{o}C prepared by (ACG).

Fig.9. The absorption coefficient (α) of ZnO (NRs) prepared at 3 different temperature150, 250 and 300^{o}C by (ACG).

Fig.10. $(\alpha h\nu)^2$ as a function of photon energy for the ZnO nanorod thin films annealed at different temperature at 150 , 250 and 300^{o}C, respectively.

Fig. 11. Calibration curve of the electrochemical potential difference, for the gold coated glass substrate ZnO (NRs) as potentiometric electrode with Ag/AgCl reference electrode versus Logarithmic concentration range for Fe^{3+} change for buffer solution.

Fig. 12. Calibration curve of the electrochemical potential difference, for gold coated glass substrate ZnO (NRs) as potentiometric electrode with Ag/AgCl reference electrode versus Logarithmic concentration range for Fe^{3+} change for Hemoglobin solution.

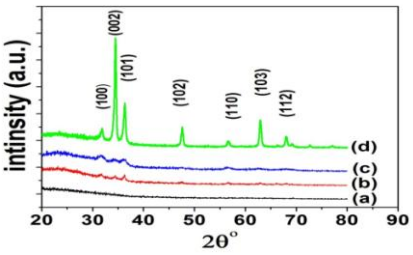

Fig. 1. (a, b,c & d) XRD of ZnO nano-particles (seed layer) before the growth of (NRs) prepared by spin coating sol gel method, heated at different temperature 100 (a), 150 (b), 250^{o}C (c), respectively. typical XRD of ZnO (NRs) prepared by aqueous chemical growth at 90^{o}C(d)

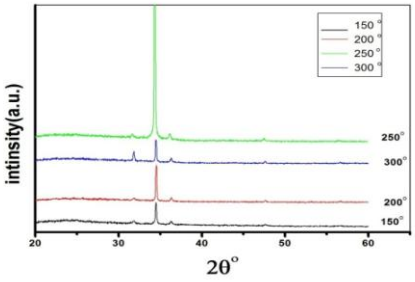

Fig. 2. XRD patterns of the ZnO NRs thin films prepared on seed layers under different annealing temperatures.

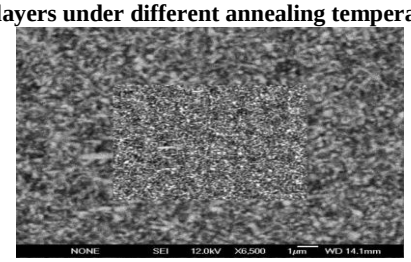

Fig. 3. Typical scanning electron microscopy (SEM) images of ZnO nano-rods grown on glass substrate, with seed layers at annealing temperature 150o C.

ISSN: 2277-3754
ISO 9001:2008 Certified
International Journal of Engineering and Innovative Technology (IJEIT)
Volume 4, Issue 1, July 2014

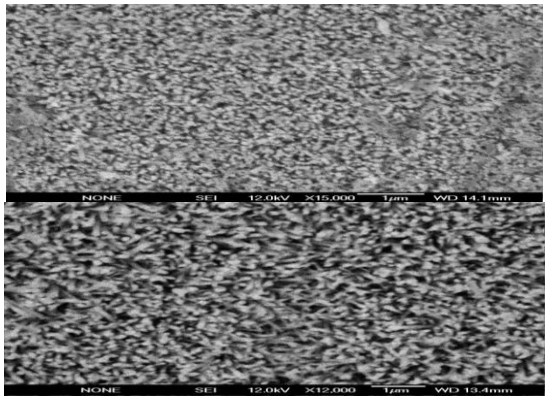

(a) (b)

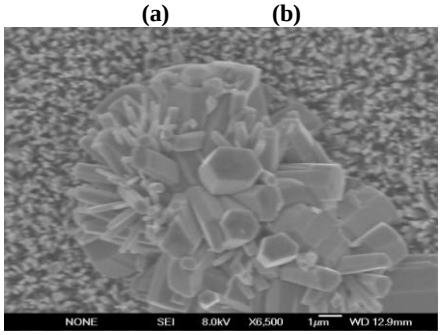

(c)

Fig.4. Typical scanning electron microscopy (SEM) images of ZnO nano-rods grown on glass substrate, with seed layers at annealing temperature 250o C (a) 3 layers (b) 6 layers and (c) 6 layers to focus on the hexagonal structure.

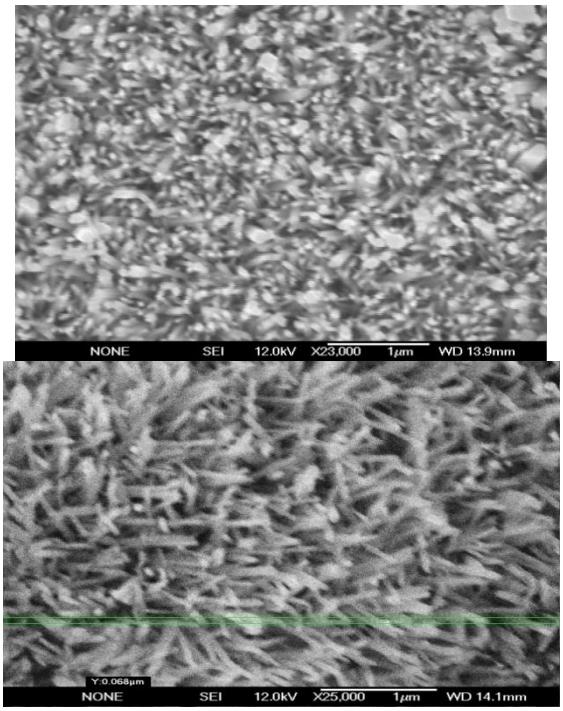

(a) (b)

Fig.5. Typical scanning electron microscopy (SEM) images of ZnO nano-rods grown on glass substrate, with seed layers at annealing temperature 300^{o} C (a) 3 layers (b) 6 layers.

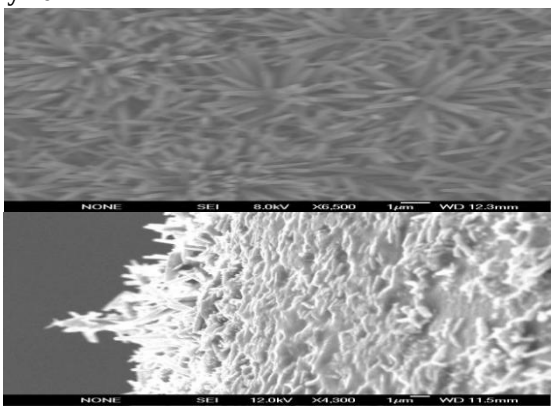

(a) (b)

Fig. 6. Typical scanning electron microscopy (SEM) images of ZnO nano-rods grown on gold coated glass substrate (a) before coating with iron membrane, (b) after coating with iron membrane.

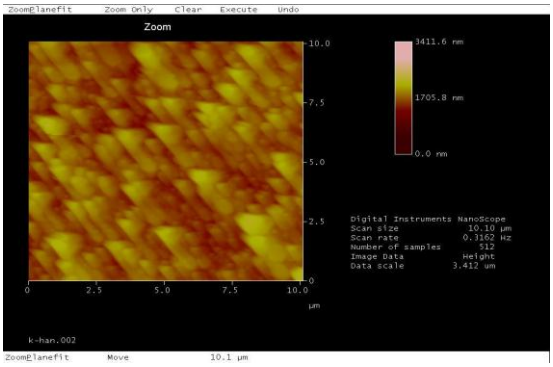

(a)

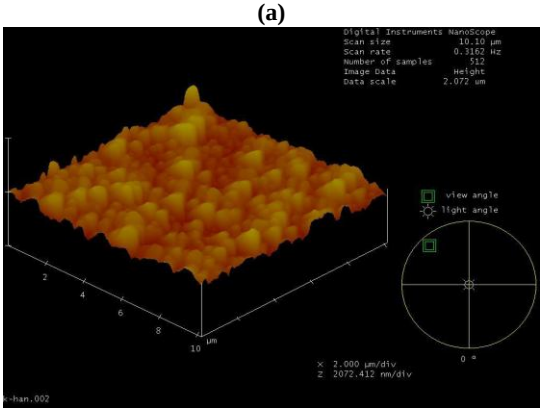

(b)

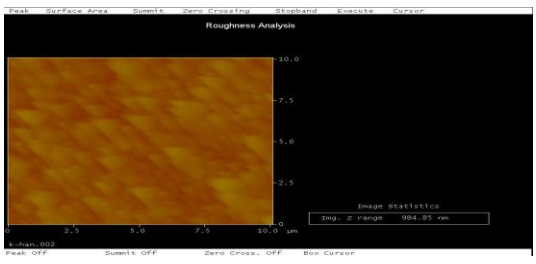

(c)

Fig.7. AFM images of ZnO (NRs) prepared by low temperature (ACG) method.

ISSN: 2277-3754
ISO 9001:2008 Certified
International Journal of Engineering and Innovative Technology (IJEIT)
Volume 4, Issue 1, July 2014

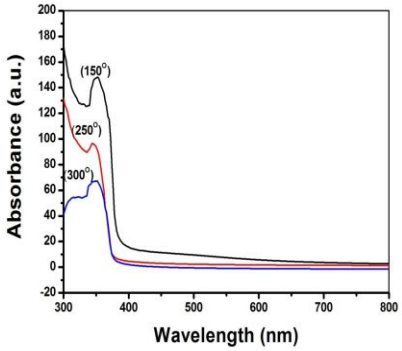

Fig.8. The absorbance of the ZnO (NRs) prepared at different temperature 150, 250 and 300°C prepared by (ACG).

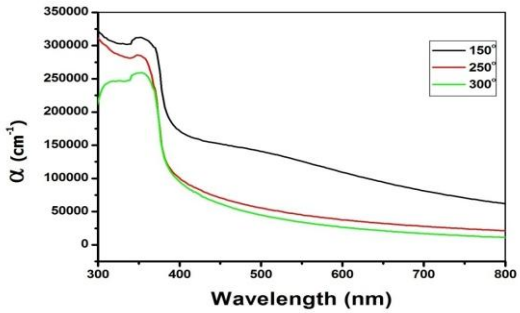

Fig.9. The absorption coefficient (α) of ZnO (NRs) prepared at 3 different temperature150, 250 and 300°C by (ACG).

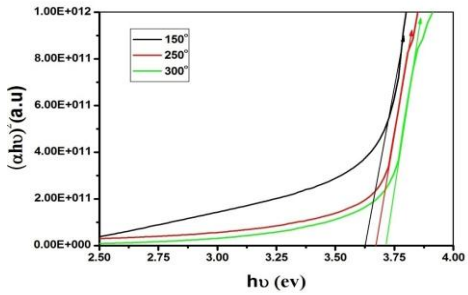

Fig.10. $(\alpha h\nu)^2$ as a function of photon energy for the ZnO nanorod thin films annealed at different temperature at 150 , 250 and 300°C,respectively.

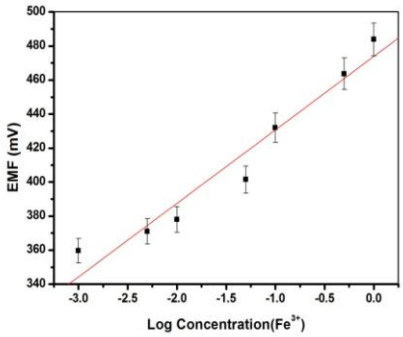

Fig. 11. Calibration curve of the electrochemical potential difference, for the gold coated glass substrate ZnO (NRs) as potentiometric electrode with Ag/AgCl reference electrode versus Logarithmic concentration range for Fe^{3+} change for buffer solution.

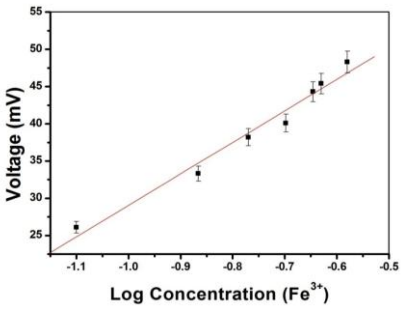

Fig. 12. Calibration curve of the electrochemical potential difference, for gold coated glass substrate ZnO (NRs) as potentiometric electrode with Ag/AgCl reference electrode versus Logarithmic concentration range for Fe^{3+} change for Hemoglobin solution.